Influence of local lattice structure on magnetic properties in Y_2Fe_{17} compounds

Jun-ichiro Inoue,[1,2] Takuya Yoshioka,[1,3,4] and Hiroki Tsuchiura[1,3,4]
[1]*Department of Applied Physics, Tohoku University, Sendai 980-8579, Japan*
[2]*Institute of Applied Physics, University of Tsukuba, Tsukuba 305-8573, Japan*
[3]*Elements Strategy Initiative Center for Magnetic Materials, National Institute for Materials Science, Tsukuba 305-0047, Japan*
[4]*Center for Spintronics Research Network, Tohoku University, Sendai 980-8577, Japan*

(Received 28 May 2020; accepted 17 September 2020; published 4 November 2020)

A theoretical study is performed on the relation between magnetic properties and lattice structures, that is, lattice constants and local atom displacement, for rhombhedral (rh-) Y_2Fe_{17} compounds. We use real-space full-orbital tight-binding formalism to calculate electronic states. Magnetic anisotropy (MA) is calculated with high numerical accuracy by adopting a second-order perturbation for spin-orbit interaction. It is shown that the local magnetic moments of Fe atoms on 9d and 18h sites increase with increasing lattice volume. The result is attributed to the high atomic area density of these sites on the hexagonal planes. Those of Fe atoms on the other sites are found to be nearly independent of the volume. We calculate local MA energy of Fe atoms on each nonequivalent site and find that the magnitude of the local MA is strongly affected by the local atom displacement. As a result, the MA of Y_2Fe_{17} is shown to be sensitive to volume.

DOI: 10.1103/PhysRevMaterials.4.114404

I. INTRODUCTION

$Sm_2Fe_{17}N_3$ [1] is known as one of the highest performance permanent magnets discovered after $Nd_2Fe_{14}B$ [2–4]. Magnetic properties, such as saturation magnetization M_s, Curie temperature T_C, and uniaxial magnetic anisotropy (MA) energy K_u, are strongly enhanced by nitrogenation of Sm_2Fe_{17} [5,6]. Many experimental and theoretical studies have been performed on the fundamental magnetic properties and electronic states of $Sm_2Fe_{17}N_x$ ($x = 0$–3) and related compounds. Nevertheless, there remain issues to be elucidated, such as the ionic and magnetic states of Sm ions [7–10] and the effects of nitrogenation on the enhancement of M_s, T_C, and K_u.

Because the quantities M_s, T_C, and K_u are closely related to the magnetic properties of Fe atoms in the compounds, the study of those in Y_2Fe_{17} and related compounds would be interesting. Figure 1 shows the relations between the lattice constant a and physical quantities such as the lattice constant c, M_s, and T_C observed for several Y_2Fe_{17} type compounds; hexagonal (h-)Y_2Fe_{17}, h-$Y_2Fe_{17}C_x$, rhombohedral (rh-)$Y_2Fe_{17}N_3$, and rh-$Sm_2Fe_{17}N_x$ [11–14]. We see that the lattice constant c is linearly proportional to the lattice constant a and that T_c increases almost linearly with the lattice constants. On the other hand, it is unclear whether the linearity holds between M_s and the lattice constants. First-principle calculations [15,16] proposed two possible interpretations for the relation between M_s and the lattice constants: one is the volume effect and the other is the nitrogenation effect [17].

The large K_u value of $Sm_2Fe_{17}N_3$ is surely related to Sm ions; however, the enhancement of M_s of Fe atoms caused by nitrogenation of Sm_2Fe_{17} could also be related to the enhancement of K_u value. Thus far, few studies have focused on the volume effect on MA energy of Fe atoms. X-ray diffraction (XRD) measurements for $Sm_2Fe_{17}N_x$ and $Y_2Fe_{17}N_x$ have revealed that local atom displacement occurs for Fe atoms in these compounds [5,12–14], as shown in the next section. The effects of the displacement of Fe atoms on magnetic properties have been discussed for $Sm_2Fe_{17}N_x$ [18]. It is known that MA energy of transition metal atoms/ions in compounds and oxides is generally affected by local atomic/ionic arrangements. In fact, we have recently reported the dependence of MA energy on oxygen displacements in h-ferrites [19,20], which are similar to the Fe displacements in Y_2Fe_{17} type compounds. Although the influence of atomic displacement on MA per atom/ion in metallic systems might be weaker than that in oxides, the influence on total MA energy per unit volume could be large in Y_2Fe_{17} compounds because of the high atomic density of Fe atoms in Y_2Fe_{17} compounds. In fact, the values of $K_u = 11$ and 7 Merg/cm^3 for $Y_2Fe_{14}B$ and $La_2Fe_{14}B$, respectively [4], are larger than the 3 Merg/cm^3 of Sr-ferrite [21]. Therefore, detailed calculations to clarify the effects of local atom displacement on the MA energy in Y_2Fe_{17} type compounds are desirable. Because the local atom displacement is correlated with the lattice expansion, these two effects must be simultaneously studied in the calculation of MA energy.

The purpose of this work is to clarify effects of lattice expansion and local displacement of Fe atoms on the electronic states and local magnetic properties, including local MA, of Fe atoms in Y_2Fe_{17} compounds. Because the MA energy of Y_2Fe_{17} type compounds is of the order of 10 Merg/cm^3 (1 Merg $= 10^6$ erg), which corresponds to 0.01 mRy per ion on average, high numerical accuracy must be achieved in the calculation to clarify the change in MA energy caused by atom displacement. Therefore, we adopt the real-space full-orbital tight-binding (TB) model to calculate the electronic states and MA energy of Fe atoms. We use a second-order perturbation for the spin-orbit interaction (SOI) to calculate MA energy

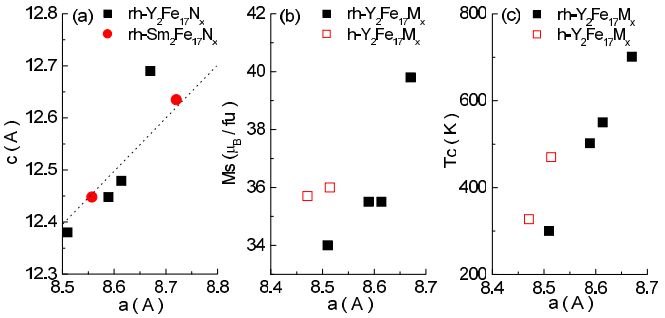

FIG. 1. Relation between observed lattice constants and magnetic properties of h-Y_2Fe_{17}, h-$Y_2Fe_{17}C_x$, rh-$Y_2Fe_{17}N_3$, and rh-$Sm_2Fe_{17}N_x$. (a) Relation between the lattice constants a and c, (b) saturation magnetization M_s, and (c) Curie temperature T_C as a function of lattice constant a.

[22,23]. We will show that the change in the lattice constants affects the local density of states (DOS) and local magnetic moments of Fe atoms mainly on c planes with high atomic area density. We further show that the local MA energy is intricately dependent on both lattice constants and Fe displacement.

In Secs. II and III we explain the lattice structure of rh-Y_2Fe_{17} and the method of calculation, respectively. In Sec. IV we show the results calculated for $Y_2Fe_{14}B$ and h-Y_2Fe_{17} and compare them with previous results. Section V gives calculated results of electronic states and magnetic properties of rh-Y_2Fe_{17} with two different lattice constants. The effects of lattice constants and atomic displacement on the magnetic properties including MA are surveyed in detail in Sec. VII. Section VII and the final section present discussions and a summary of our work, respectively.

II. LATTICE STRUCTURE

Two types of lattice structure exist for Y_2Fe_{17} compounds [5]; one is a hexagonal Th_2Ni_{17} type, which contains two formula units (fu's) in one unit cell (uc), and the other is a rhombohedral Th_2Zn_{17} type, which contains three fu's in one uc. Figure 2 shows the configuration of atoms on each c plane in rh-Sm_2Fe_{17} obtained in the x-ray diffraction (XRD) experiment [13]. Positions of the c planes along the c axis are given by the values of z in the figure. There are five nonequivalent sites in rh-Y_2Fe_{17}: 6c(Y), 6c(Fe), 9d(Fe), 18f(Fe), and 18h(Fe), while h-Y_2Fe_{17} contains six nonequivalent sites: 2b(Y), 2d(Y), 4f(Fe), 6g(Fe), 12j(Fe), and 12k(Fe). In Fig. 2, possible sites for N are also presented by crosses for discussion.

Constituent Y and Fe atoms reside basically on the hexagonal lattice points; however, several Fe atoms are displaced from the hexagonal lattice points. It is shown in Fig. 2 that 18f(Fe) sites are shifted on c planes as indicated by arrows. The lattice constants and magnitude of displacement δx of Fe atoms of several compounds are summarized in Table I. We see that displacement is nonzero even in compounds without N, which is attributed to the large atomic radii of Y and Sm and that the displacement increases further by introduction of N.

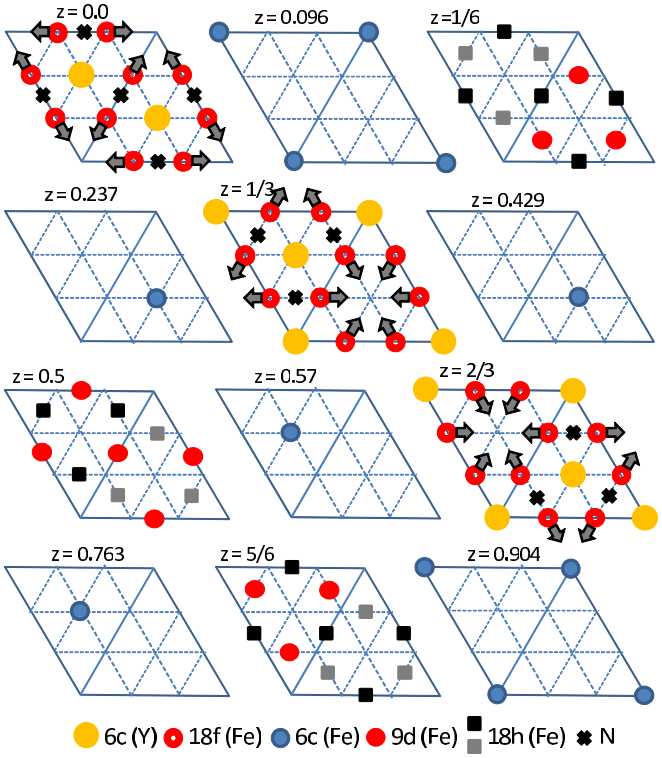

FIG. 2. Atomic positions on c planes in rh-Sm_2Fe_{17} observed by XRD [13]. Positions of the planes along the c axis are given by the values of z in the figure. 18f(Fe) sites are shifted from the hexagonal lattice points, as shown by arrows. Sites that can host N are also indicated by crosses for convenience. Lattice constants are $a = 8.557$ Å and $c = 12.448$ Å.

It may be noted that vertical displacements also occur for the 18h(Fe) and 6c(Y) sites along the c axis [13]. However, the magnitude of the shift δz is small, i.e., ± 0.0113 and ± 0.0097 in units of c for 18h(Fe) and 6c(Y), respectively, and may have only minor effects on the magnetic properties.

III. METHOD OF CALCULATION

We apply a full-orbital 3d-TB model to calculate the electronic states of Y_2Fe_{17} compounds. The Hamiltonian is given

TABLE I. Lattice constants and magnitude of displacements of Fe(18f) atoms in rh-Y_2Fe_{17} type compounds. The hexagonal coordinate is adopted, and the displacement along $x(y)$ axis is given in units of the lattice constant a.

Material	a (Å)	c (Å)	$\lvert\delta x\rvert = \lvert\delta y\rvert$	Ref.
Y_2Fe_{17}	8.500	12.429	0.0379	[12]
$Y_2Fe_{17}N_{3.1}$	8.671	12.724	0.0504	[12]
Sm_2Fe_{17}	8.557	12.448	0.0443	[13]
$Sm_2Fe_{17}Ga_2$	8.606	12.521	0.0443	[13]
$Sm_2Fe_{17}N_3$	8.721	12.635	0.0507	[14]

as

$$\boldsymbol{H} = \boldsymbol{H}_0 + \boldsymbol{H}_{\rm SO}, \tag{1}$$

$$\boldsymbol{H}_0 = \sum_{i\neq j,\sigma,\mu,\nu} T_{ij}^{\mu\nu} c_{i\sigma\mu}^{\dagger} c_{j\sigma\nu} + \sum_{i,\sigma,\mu} V_{i\sigma}^{\mu} c_{i\sigma\mu}^{\dagger} c_{i\sigma\mu}, \tag{2}$$

$$\boldsymbol{H}_{\rm SO} = \xi \boldsymbol{s}\cdot\boldsymbol{l}, \tag{3}$$

where $\boldsymbol{H}_{\rm SO}$ is the spin-orbit interaction (LS coupling), $T_{ij}^{\mu\nu}$ represents electron hopping between site i with μ orbital and site j with ν orbital, $V_{i\sigma}^{\mu}$ gives a spin(σ)-dependent diagonal potential for electrons at site i, and $c^{\dagger}$ and c are creation and annihilation operators, respectively. Adopting the Hartree-Fock approximation for the exchange interaction between electrons, we take

$$V_{i\sigma}^{\mu} = V_i + U_i \langle n_{i\bar{\sigma}} \rangle, \tag{4}$$

where $\langle n_{i\bar{\sigma}} \rangle$ is an expectation value of electron number on site i with spin $\bar{\sigma}$, and V_i and U_i are the atomic potential and exchange interaction on the ith site, respectively. The quantity $\langle n_{i\bar{\sigma}} \rangle$ will be determined self-consistently. Here we neglect the orbital dependence of $V_{i\sigma}^{\mu}$. In the following we assume that $V_i(U_i)$ takes $V_{\rm Y}(U_{\rm Y})$ or $V_{\rm Fe}(U_{\rm Fe})$.

There are several parameters whose values should be determined in advance: the matrix elements $T_{ij}^{\mu\nu}$ are determined by the framework given by Harrison's textbook [24], and we take $V_{\rm Y} \equiv 0$ and $V_{\rm Fe} = -0.5$ Ry to satisfy the $3d$-electron number of Y and Fe observed in metallic states, that is, $n_{\rm Y} = 1.65$/atom and $n_{\rm Fe} = 7.4$/atom, respectively [23,25,26]. We further assume $U_{\rm Y} = 0$ and take $U_{\rm Fe}$ as an adjustable parameter of approximately 0.07 Ry. It may be noted that $U_{\rm Fe} \sim 0.06$ Ry for bcc Fe. The magnitude of the SOI is taken to be 2 and 4 mRy for Fe and Y, respectively [20,27]. Note that the value of SOI is ambiguous; values of approximately 4–5 mRy are given for Fe ions [27], and a similar value was estimated for Fe atoms in $L1_0$-FePt alloy [28]. On the other hand, we used 1.5 mRy for Co^{2+} ions in spinel and hexagonal ferrites to explain the experimental results of MA energy [20].

The electronic states are determined by calculating the Green's function $\boldsymbol{G}$ defined as $\boldsymbol{G} = [E + i0 - \boldsymbol{H}]^{-1}$ by applying the real-space recursive method [29] for finite size clusters which contains approximately 7000 atoms [22,25,26]. Self-consistent calculations for $\langle n_{i\sigma} \rangle$ are performed, and local and total density of states (DOS) and Fermi energy ε_F are determined simultaneously.

The MA energy is calculated in the second-order perturbation in the following way. We consider the thermodynamic potential at 0 K:

$$\Omega = E_{\rm T} - N\mu = \int_{-\infty}^{E_F} (E - E_F)\rho(E)dE, \tag{5}$$

where $E_{\rm T}, N$, and μ are total energy, total electron number, and chemical potential (i.e., Fermi energy at 0 K) for d electrons, respectively. Ω can be expressed as

$$\Omega = -\frac{1}{\pi}\int_{-\infty}^{E_F} {\rm Im\,Tr\,ln}\boldsymbol{G}(E)dE. \tag{6}$$

TABLE II. Present results are compared with previous theoretical as well as experimental results for $Y_2Fe_{14}B$. Values $U_{\rm Fe} = 0.07$ Ry and $V_{\rm Fe} = -0.47$ Ry are used in the present calculation.

		M_s ($\mu_{\rm B}$/fu)	K_u (Merg/cm^3)
Expt.		31.4	11
		29.5	–
Calc.	first principles [35]	32.05	4.4
	first principles [34]	30.47	–
	previous TB [34]	–	11.4
	present TB-HF	33.05	3.4

We expand Ω up to the second order of SOI $\boldsymbol{H}_{\rm SO}$ [30], resulting in

$$\Delta\Omega \equiv \Omega - \Omega_0 = -\frac{1}{2\pi}\int_{-\infty}^{E_F} {\rm Im\,Tr}(\boldsymbol{H}_{\rm SO}\boldsymbol{g})^2 dE, \tag{7}$$

where $\boldsymbol{g} = [\varepsilon + i0 - \boldsymbol{H}_0]^{-1}$. The first order term of $\boldsymbol{H}_{\rm SO}$ vanishes identically. The trace is taken over sites, orbitals, and spins.

The dependence of $\Delta\Omega$ on the direction of the magnetic moment is included in the matrix elements of $\boldsymbol{H}_{\rm SO}$ as polar angles (θ, φ) [31]. When $\varphi = 0$, Eq. (7) gives $\Delta\Omega = K_u \sin^2\theta$, where K_u is the uniaxial MA energy. Note that $K_u \sim K_1 + K_2$ in general, where K_1 and K_2 are the anisotropy constants, and that the present scheme excludes the contribution of K_2 which is proportional to the fourth order of $\boldsymbol{H}_{\rm SO}$. K_u is given by a sum of local MA $K_u^{(i)}$ of Fe atoms on the nonequivalent site i. There are two contributions to $K_u^{(i)}$; one is from intrasites for which the intrasite Green's functions g_{ii}^{σ} and $g_{ii}^{\sigma'}$ contribute, and the other is from intersites for which the off-diagonal ones g_{ij}^{σ} and $g_{ji}^{\sigma'}$ contribute. The intra- and intersite Green's functions are calculated by using the symmetry conserving recursive method [32,33]. In the practical calculations, up to the third nearest neighbor (n.n.) sites are taken into account for the intersite contributions. In the recursive method, the Green's functions are represented by continued fractions, coefficients which are expressed by 5×5 matrices and calculated numerically up to the Lth level ($L = 12$ or 20 in the present calculations).

IV. COMPARISON WITH PREVIOUS RESULTS

In this section we compare calculated results for $Y_2Fe_{14}B$ and h-Y_2Fe_{17} with previous ones. Calculated results of M_s and K_u for $Y_2Fe_{14}B$ are compared in Table II with experimental and previous theoretical results [34,35]. The lattice constants are $a = b = 8.792$ Å and $c = 12.190$ Å. The contribution of B atoms was neglected. Vienna *ab initio* simulation package (VASP) was used for the first principles, and a non-self-consistent method was used in the previous TB method instead of the present self-consistent TB-HF method.

We find that the present result of M_s is slightly larger than the experimental ones, and the value of K_u is smaller than the experimental one. The value of K_u is consistent with that obtained in the first principles. The large K_u value in the previous TB calculation is due to the large SOI value of 5 mRy assumed in the calculation.

TABLE III. Present results of M_s and K_u of h-Y_2Fe_{17} calculated in the TB-HF formalism and experimental results of M_s [11,12,36,37] and $K_u = K_1 + K_2$. In the calculations, two sets of lattice constants, S-lc and L-lc, were used (see text). For comparison, experimental values of M_s [12] and K_u of rh-$Y_2Fe_{17}N_3$ are also presented.

		M_s (μ_B/fu)	K_u (mRy/fu)	K_u (Merg/cm^3)
Expt.	h-Y_2Fe_{17}	34–36	−0.30	−25 [38]
			−0.35	−29 [39]
	rh-$Y_2Fe_{17}N_3$	40	−0.18	−15 [38]
Calc.	S-lc	36.24	−0.0075	−0.63
	L-lc	41.34	−0.158	−12.3

As for h-Y_2Fe_{17}, calculations were performed for two sets of lattice constants: small lattice constants (S-lc), $a = 8.478$ Å and $c = 8.304$ Å, and large lattice constants (L-lc), $a = 8.74$ Å and $c = 8.43$ Å. The former values are those used in our previous study [25], which are close to observed values [11]. The latter values of a and c are the same for a and 2/3 of c in rh-$Sm_2Fe_{17}N_{3.1}$ [12]. As for the local shift of Fe atoms, we adopt the same magnitude as that of rh-Sm_2Fe_{17} shown in Table I. The values of U_{Fe} and V_{Fe} are 0.07 and −0.5 Ry, respectively.

Table III presents the calculated results of M_s and K_u and experimental ones. Note that the experimental values of K_u is $K_1 + K_2$, and that Table III includes experimental values of rh-$Y_2Fe_{17}N_3$ for comparison. Discussion on calculated results for rh-Y_2Fe_{17} will be given in Sec. VII. The calculated value of M_s for S-lc is nearly the same as the experimental one, and it increases for L-lc. The sign of K_u is negative, indicating that h-Y_2Fe_{17} shows in-plane MA, and the magnitude depends strongly on the volume.

To clarify the mechanism of the increase in M_s shown in Table III, in Table IV we compare the calculated values of local magnetic moments on nonequivalent sites in the present method with those in the previous first principles [15]. We find that the present results agree well with the previous ones and that the local magnetic moments on Fe(6f) and Fe(12k) increase with increasing lattice constants.

Thus, the present TB-HF method may reproduce the previous results adequately. In the next section we survey the mechanism of the enhancement of the local magnetic moments with lattice expansion and clarify possible relations among the lattice structure, electronic states, and magnetic properties.

TABLE IV. Comparison between the local magnetic moments (in units of μ_B/atom) calculated by the present method with those calculated by the linear muffin tin orbital (LMTO) method [15].

		Y (2b)	Y (2d)	Fe (4f)	Fe (6g)	Fe (12j)	Fe (12k)
LMTO	S-lc	−0.47	−0.45	2.53	1.92	2.25	2.00
	L-lc	−0.20	−0.45	2.65	2.53	2.01	2.57
Present	S-lc	−0.36	−0.41	2.65	1.97	2.46	1.85
	L-lc	−0.39	−0.48	2.61	2.64	2.54	2.31

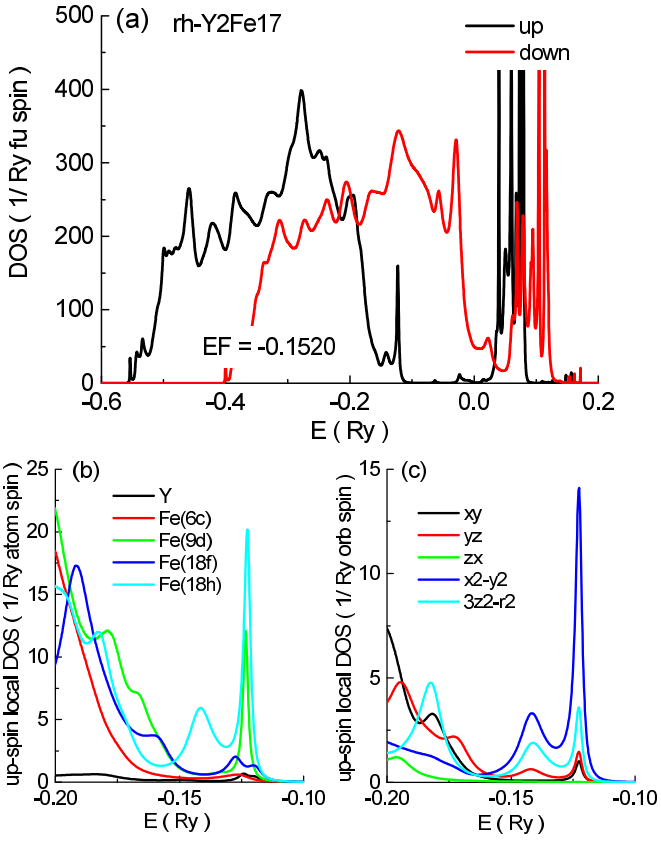

FIG. 3. Calculated results for (a) total DOS of rh-Y_2Fe_{17}, (b) local DOS of each nonequivalent site, and (c) orbital decomposed DOS of the total DOS. The lattice constants and local lattice structure shown in Fig. 2 are used. The Fermi energy $E_F = -0.152$ Ry.

V. RESULTS FOR rh-Y_2Fe_{17}

A. Electronic states

We first show calculated results of the electronic states of rh-Y_2Fe_{17} in Fig. 3. We use the values of lattice constants and atomic displacement observed for rh-Sm_2Fe_{17} shown in Fig. 2 as a typical example.

Calculated results of 3d-DOS of up and down spin states are shown in Fig. 3(a). The states below $E \lesssim 0$ Ry are mainly composed of Fe 3d states, and peak states at high energy originate mainly from Y 4d states. The Fermi energy is located at $E_F = -0.152$ Ry. It is notable that there exists a small but sharp peak just above the up-spin 3d states near $E \sim -0.1$ Ry.

Figure 3(b) shows the local DOS of the nonequivalent sites near E_F. We find that the sharp peak near $E \sim -0.1$ Ry originates mainly from Fe(18h) and Fe(9d) atoms. The result is consistent with that calculated previously by the LMTO method for rh-Y_2Fe_{17} by Coehoorn [40,41], where lattice constants $a = 8.46$ Å and $c = 12.41$ Å were used. These values are slightly smaller than those used in the present calculations. In his results, the Fermi energy is located within the up-spin 3d states but close to the top of the 3d states, and there exist shoulders of local DOS of Fe(9d), Fe(18h), and Fe(18f) at the

Fermi energy. The height of the local DOS of the Fe(18f) atom at the Fermi energy is approximately half that of the other two local DOS. The present results shown in Fig. 3(b) are consistent with his results when we consider a broadening of the peak caused by *s*-*d* and *p*-*d* hybridizations, which were neglected in our method. It should be noted that the results obtained by Jaswal *et al.* [15] also show the same tendency.

Figure 3(c) presents orbital decomposed DOS near E_F. We see that the largest contribution to the peak comes from the $d_{x^2-y^2}$ component.

To interpret the calculated results shown in Fig. 3, let us consider the local lattice structure shown in Fig. 2. The Fe(9d) and Fe(18h) atoms are located on the same *c* plane, for example at $z = 1/6$, in the figure. The Fe(6c) and Fe(18f) atoms are located on different planes. Because the *c* plane at $z = 0$, on which Y(6c) and Fe(18f) reside, contains six Fe atoms on a single rhombus, while the plane at $z = 1/6$, on which Fe(9d) and Fe(18h) reside, contains nine Fe atoms. This means that the atomic area density is higher on the $z = 1/6$ plane than on the $z = 0$ plane. The difference may be caused by the large atomic radius of Y.

Interatomic distance in rh-Y_2Fe_{17} was investigated in detail experimentally [12]. The results show that the interatomic distances of Fe(18h)-Fe(18h) and Fe(18h)-Fe(9d) bonds are short with high multiplicity, and the average interatomic distances for Fe(9d) and Fe(18h) are also short. The short atomic distance makes *d*-*d* hopping between n.n. Fe sites large, resulting in wide local DOS for Fe(9d) and Fe(18h). Such an effect may be largest for the *d*-*d* hopping between $d_{x^2-y^2}$ orbitals. Thus, the sharp peak existing just above the up-spin 3*d* states is a split-off state from the main up-spin 3*d* states caused by dense packing of Fe(9d) and Fe(18h) atoms.

B. Magnetic properties

To compare the calculated results with experimental ones, we perform calculations for rh-Y_2Fe_{17} with two sets of lattices constants: small lattice constants (S-lc) and large lattice constants (L-lc) observed for rh-Y_2Fe_{17} and rh-$Y_2Fe_{17}N_x$, respectively [12]. Note that these lattice constants are different from those of rh-Sm_2Fe_{17} used for Fig. 3. The values of the lattice constants and in-plane displacements of Fe(18f) are shown in Table I. The value of U_{Fe} is taken to be 0.075 Ry in the calculations. Figures 4(a), 4(b) 4(c), and 4(d) show calculated results of saturation magnetization M_s, local magnetic moments, local MA energy, and local DOS, respectively. In Fig. 4(d), local DOS of Fe(9d), Fe(18f), and Fe(18h) atoms are presented for discussion, where thick (thin) curves are the result for small (large) lattice constants.

Figure 4(a) shows dependence of M_s on the lattice constants. The theoretical values increase with increasing lattice constants. The origin is attributed to the shift of the peak of the up-spin 3*d*-DOS caused by the change in the lattice constants, as discussed in the previous subsection. The shifts of the local DOS peaks near the Fermi energy (E_F) are shown in Fig. 4(d) for Fe(9d), Fe(18f), and Fe(18h) atoms. Thus, the increase in M_s is due to the change in the up-spin DOS.

The theoretical increment in M_s shown in Fig. 4(a), however, is nearly half of the experimental one [12]. The reason for the difference can be seen in Fig. 4(b), where the results of

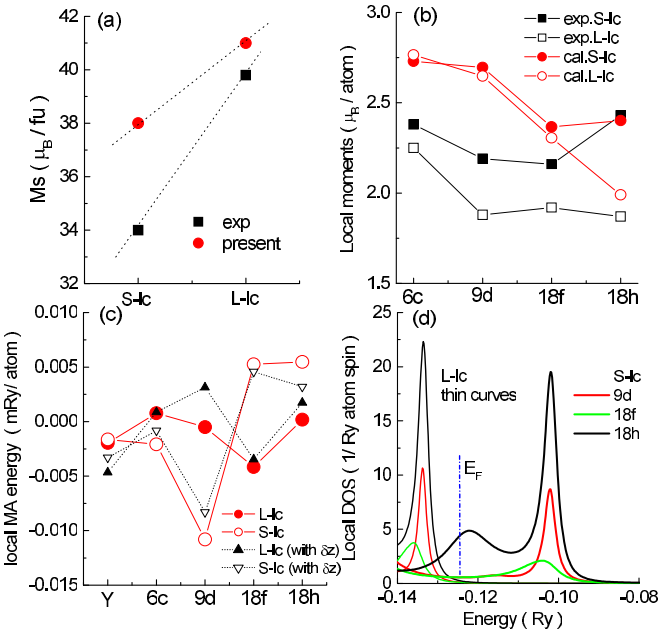

FIG. 4. Calculated results for rh-Y_2Fe_{17} with small (S-lc) and large lattice constants (L-lc). (a) Saturation magnetization M_s, (b) local magnetic moments on the nonequivalent Fe sites, which are compared with observed values [12], (c) local MA energy of the nonequivalent Fe sites with and without shifts δz of Y(6c) and Fe(18h) along the *c* axis, and (d) local DOS of Fe(9d), Fe(18f), and Fe(18h). Here E_F is presented by a broken line.

the local magnetic moments of the nonequivalent Fe atoms are compared with experimental ones [12]. In the figure, circles and squares indicate the calculated and experimental values, respectively, of the local moments on the nonequivalent sites. As shown in the figure, the experimental values for L-lc are larger than those for S-lc by 0.2–0.4 μ_B/atom. On the other hand, the calculated values of the local moments on Fe atoms are nearly independent of the lattice constants except for Fe(18h) sites. In the calculation we have confirmed that the effects of atom displacement δz along the *c* axis are negligibly small for the local magnetic moments.

The change in the local magnetic moments is directly related to the change in the up-spin local DOS shown in Fig. 4(d). We find that the change in the local DOS is the largest for the Fe(18h) site, which is closely related to the fact that Fe(18h) sites are located on *c* planes with high atomic area density, as discussed. Note that the position of E_F is nearly independent of the lattice constants.

The calculated results of the local magnetic moments shown in Table IV for h-Y_2Fe_{17} are also understood in the same way because Fe(6g) and Fe(12k) sites in h-Y_2Fe_{17} are located on the *c* planes with high atomic area density, and the local lattice structure is basically the same as that on the *c* plane at $z = 1/6$ in rh-Y_2Fe_{17}. Previous LMTO calculations [40] showed that the local DOS peak may exist for Fe(9d) sites. However, the present results show that the moment of the Fe(9d) site is nearly independent of the lattice constants. This discrepancy might be attributed to the difference in the values of the lattice constants used in the calculations, which will be discussed in the next subsection.

The present results could not explain all the experimental results for the dependence of the local magnetic moments on the lattice constants. We therefore presume that the observed change in the local moments of Fe(6c) and Fe(18f) atoms may be caused by nitrogenation, which is not taken into account in our calculations. Actually, these sites are close to N atoms and charge transfer from the down-spin Fe states to N may occur easily.

So far we have shown that the change in the local magnetic moments with lattice constants depends on the position of Fe sites. It is noted, however, that the consequence can be modified by a different choice of U_{Fe} value: large (small) U_{Fe} makes the local magnetic moments large (small) independently of the lattice constants. Nevertheless, we believe the choice of U_{Fe} values around 0.07–0.075 Ry is acceptable in view of the reasonable agreement of the present results with those in the previous LMTO calculations.

Now, let us discuss the results for the MA energy. Calculated values of MA energy per fu are -0.0278 mRy (-2.20 Merg/cm^3) and 0.0245 mRy (2.06 Merg/cm^3) for L-lc and S-lc, respectively. Although the magnitude of these values is the same order of that calculated for $Y_2Fe_{14}B$ and h-Y_2Fe_{17}, the sign of the MA energy is dependent on the lattice constants. Furthermore, the magnitude of the MA energy calculated for rh-Y_2Fe_{17} is smaller than the experimental values of h-Y_2Fe_{17} and rh-$Y_2Fe_{17}N_3$ shown in Table III. Discussions on the disagreement will be given in Sec. VII.

The calculated results of the local MA energy are shown in Fig. 4(c). Triangles are results calculated with atomic displacement δz along the c axis. We find that the results are rather strongly dependent on the lattice constants and atomic displacement. Nevertheless, both Fe(18f) and Fe(18h) atoms may govern the sign of the MA energy, that is, their MA energy is positive (negative) for S-lc (L-lc).

The site dependence of the MA energy on the lattice constants is rather difficult to interpret, in contrast to that of the local magnetic moments. To clarify a relation between the electronic states and local MA energies (K_u values), we present the energy dependence of the local MA energies in Fig. 5. Thick (thin) curves are results for Fe(9d), Fe(18f), and Fe(18h) atoms with S-lc (L-lc). The position of the Fermi energy (E_{F}), which is almost independent of the lattice constants, is shown by a thick broken line. In the figure the positions of up-spin DOS peaks are indicated by vertical broken lines at approximately -0.10 and -0.13 Ry for S-lc and for L-lc, respectively.

We find two features in the curves of MA energy: one is that there exists a dip in the curve near the position of DOS peak for Fe(9d) and Fe(18h) sites, and the other is that shapes of the curves near the peak position for L-lc and S-lc is similar to each other. The features suggest that the local MA is also related to the local electronic structure. Further discussion will be given at the end of next section.

VI. LATTICE CONSTANTS VS ATOMIC DISPLACEMENTS

In the following we study the effects of the lattice constants and displacement of Fe atoms on magnetic properties, especially on the MA energy, in detail. We take $a = 8.4 + 0.1 \times n$ and $c = 12.3 + 0.1 \times n$ in Å with $n = 1$, 2, 3, and 4. The

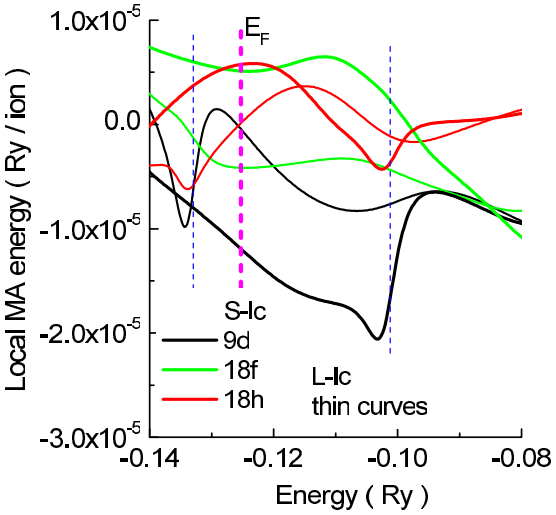

FIG. 5. Calculated results of the energy dependence of local MA energies for Fe(9d), Fe(18f), and Fe(18h) atoms with S-lc (thick curves) and L-lc (thin curves). Thin dotted lines indicate positions of DOS peaks, and the thick dotted line shows the position of Fermi energy, which is almost independent of lattice constants.

linear dependence is nearly the same as that given by the dotted line in Fig. 1(a). We prepare two sets of atomic displacement: one includes the atomic displacements, the magnitudes of which are the same with those observed for rh-Sm_2Fe_{17}, and the other does not include them. Although the displacements of Fe(18h) and Y(6c) along the c axis are included in the calculation, their effects on the magnetic properties have been confirmed to be minor.

Results for M_s, local moments of Y, and those of Fe atoms are shown in Figs. 6(a), 6(b), and 6(c), respectively. Closed and open symbols are results with and without atomic displacement, respectively. Characteristics of the results for magnetization and local magnetic moments may be summarized as follows:

(i) M_s increases monotonically with increasing a, which may be caused by the volume effect. There is almost no effect of the atomic displacement on M_s, which could be attributed to a cancellation of the change in the local moments, as shown next.

(ii) The magnitude of the local moments of Y decreases with increasing a and the inclusion of Fe displacement. This is because the d-d hybridization between Y and nearby Fe atoms becomes weak as the lattice expands and Fe displacement occurs.

(iii) As for the local moments of Fe, only the moments on Fe(18h) atoms increases with increasing a, which is attributed to the shift of the peak at the top of the up-spin DOS as mentioned. The increase in the local moments on Fe(18f) atoms with Fe displacement is caused by the decrease in the d-d hybridization between Fe(18f) and Y. The opposite tendency for the Fe(18h) moments may be due to a decrease in the distance of Fe(18h)-Fe(18f) bonds as presumed in Fig. 2. Because of the opposite tendency for Fe(18f) and Fe(18h) moments, the bulk M_s depends only weakly on the Fe displacement.

(iv) The local magnetic moments of Fe(6c) and Fe(9d) atoms are nearly independent of the lattice constant a.

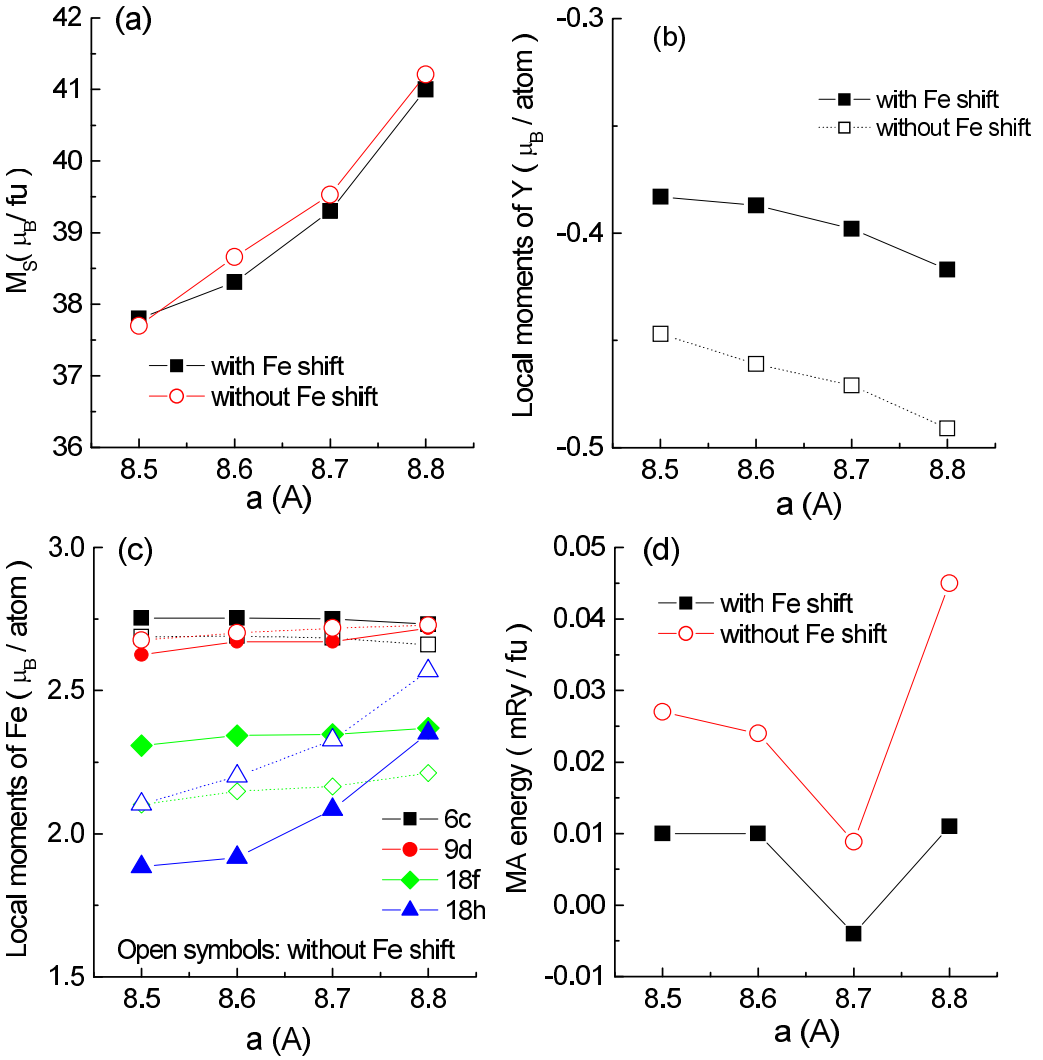

FIG. 6. Calculated results for the dependence on lattice constants of (a) saturation magnetization M_s, (b) local moments of Y, (c) local moments of nonequivalent Fe sites, and (d) MA energy per fu. Closed and open symbols are calculated results with and without local shift of Fe atoms, respectively.

However, the moment of Fe(9d) increases slightly with increasing a. This may be a result of Fe(9d) sites residing on the high atomic density planes, as mentioned in Sec. VI. Therefore, the local moments of Fe(9d) could be affected by both the volume change and nitrogenation.

The dependence of the MA energy on the lattice constant is nonmonotonic as shown in Fig. 6(d). Corresponding results for the local MA are shown in Figs. 7(a) and 7(b) with and without atomic displacement, respectively. Here we note that the numerical errors in the self-consistent calculations are smaller than 0.001 mRy. The dependence of MA on lattice constants and Fe displacement seems to be complicated and rather difficult to interpret. Nevertheless, the results shown in Figs. 6(d) and 7(a) and 7(b) indicate a common tendency for the dependence on the lattice constants. The change in the total and local MA energies for $a = 8.5$–8.7 could be gentle: however, they change rather abruptly from $a = 8.7$ to 8.8. The abrupt change is attributed to the shift of the DOS peak below the Fermi energy for $a = 8.8$. In this sense, the characteristics of the local and total MA energy may be related to the existence of a $3d$-DOS peak in the up-spin states.

The relation between the MA energy and electronic structure could be explained in the following way. So far several

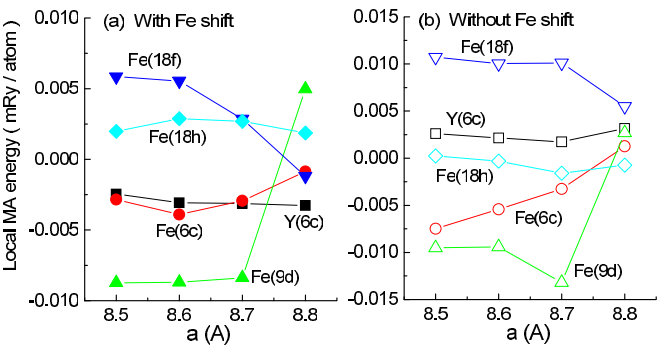

FIG. 7. Calculated results of local MA energy for various lattice constants (a) with Fe displacement and (b) without Fe displacement.

theoretical calculations of MA energy of metallic magnets have showed that the MA energy oscillates strongly as a function of energy (position of Fermi energy) [22,42,43]. It has been shown that such oscillation is explained in terms of moment expansion of physical quantities [22,44,45], and that the oscillation becomes more oscillatory when the order of the nonzero moments of the quantity in question become high. Because the MA energy depends on the distance between nearby magnetic atoms, orbitals, and the spins, the MA energy should be highly oscillatory with respect to the position of Fermi energy. As a result, the MA energy changes rapidly with the energy near the peak position.

The different dependence of the local MA energy on the lattice constants may thus be closely related to the local electronic structures. In the realistic electronic states, however, the sharp peak in the up-spin DOS may be broadened by *s*-*d* and *p*-*d* hybridization, and the strong dependence of the MA energy on the lattice constants shown in Figs. 6(d) and 7 might be weakened. Resultant MA energy could be approximately 0.01 and 0.025 mRy per fu, which correspond to 0.8 and 2 $\mathrm{Merg/cm^3}$, respectively, for the lattices with and without Fe displacement. Although these values of MA energy may not be large enough, the effect of the lattice on the MA energy is non-negligible. Careful evaluation of the MA energy, especially under nitrogenation, is desirable in various calculations, including the first principles.

VII. DISCUSSION

In previous sections we have shown that the electronic states and magnetic properties of Y_2Fe_{17} are affected rather strongly by the lattice expansion and the displacement of Fe atoms accompanied with the nitrogenation. Although the calculated results of M_s are consistent with the experimental ones, quantitative agreement between the calculated and experimental results of MA is rather poor. The calculated values of K_u for h-Y_2Fe_{17} are negative in agreement with observed ones as presented in Table III. However they depend rather strongly on the lattice constants, and the magnitude is smaller than that of the observed K_u values. The calculated values of K_u for rh-Y_2Fe_{17} are 0.01–0.045 mRy/fu as shown in Fig. 6. They are one order of magnitude smaller than the experimental values. Even the sign of K_u disagrees with the experimental one. In the following we discuss possible reasons for the disagreement and related issues.

There may be several reasons for the disagreement between the theoretical and experimental results of K_u; one is attributed to the approximation and the ambiguity of parameter values used in our model, and the others are effects neglected intrinsically in the present model.

We used a second-order perturbation for the spin-orbit interaction, and assumed the *d*-electron numbers of Fe and Y. The second-order perturbation is surely suitable for metals with weak MA except for those with cubic symmetry. Although Y_2Fe_{17} compounds are metallic, however, the MA energy is rather large as listed in Table III. Thus the second-order perturbation could be a source of the disagreement. The quantitative values of MA energy in metallic systems are dependent on the number of electrons, that is on the position of Fermi energy, because MA energy oscillates with occupation number of *d* electrons [22,42,43]. Therefore, the assumption on the *d*-electron number could be another source of the disagreement. The approximation and assumption in the present method, however, might not affect seriously to the MA energy because the similar calculations for $Y_2Fe_{14}B$ have given reasonable results as shown in Table II.

The intrinsic effects neglected in the present model are the nitrogenation and orbital polarization. Hybridization between *d* states of Fe and *p* states of N atoms should affect the MA energy in rh-$Y_2Fe_{17}N_3$. However, the effect may not be enough to explain the disagreement for rh-Y_2Fe_{17} which contains no N atoms. As for effects of the orbital polarization, intensive studies have been performed for YCo_5 in the first principles [46–49]. It has been shown that inclusion of the orbital polarization substantially enhances the MA energy resulting in a rather good agreement between the theoretical and experimental values. The orbital moments of Co atoms are also enhanced by the orbital polarization, however, the calculated values of the orbital moments are still smaller than the experimental ones especially for Co on 2c site [50]. It is also interesting to note that results of the anisotropy of the orbital moments calculated in the first principles with the orbital polarization [47–49] agree reasonably with experimental ones [51]. Especially Yamaguchi *et al.* [48] showed that the anisotropy of the orbital moments is nearly proportional to the MA energy for a series of Y-Co compounds in accordance with the suggestions by Bruno [52] and Dürr and van der Laan [53]. Thus, inclusion of the effects of nitrogenation and orbital polarization may improve the present results for Y_2Fe_{17} and $Y_2Fe_{17}N_3$. It is also interesting to note that the K_u value of Y_2Fe_{17} is nearly one order of magnitude larger than that of Y_2Co_{17} [54]. Large magnetovolume effect in Y-Fe compounds [11] might be crucial for the large MA in Y_2Fe_{17}.

Finally, let us mention the lattice effects on the electronic states in Y compounds with transition metal elements. In the present work we showed that the lattice expansion may alter the electronic states resulting in a change in the magnetic properties. A similar effect has been reported for YCo_5 compound both experimentally and theoretically [55]; high hydrostatic pressure produces a first-order transition to destroy the strong ferromagnetism in YCo_5. The phenomenon has been attributed to peculiar electronic states of Co-3*d* states [56]. Relations among the change in the electronic states, MA energy, and magnetovolume effect in Y-Co and Y-Fe compounds would be another interesting subject to be studied in future.

VIII. SUMMARY

To clarify the relation between the magnetic properties and lattice structure, we performed real-space TB-HF calculations for rh-Y_2Fe_{17} compounds. The spin-orbit interaction was treated by second-order perturbation, and the numerical accuracy for the magnetic anisotropy is therefore sufficiently high. The present method reproduced previous theoretical results reasonably well, indicating the validity of the method.

We have found that a split-off peak appears just above the up-spin local DOS for Fe(9d) and Fe(18h) consistently with the previous LMTO calculations. This is because these Fe sites reside on the same *c* planes with high atomic area

density and are strongly affected by change in the lattice constants. When the lattice expands, the *d*-*d* hopping between Fe atoms on the *c* plane becomes small, and the 3*d* bands shrink resulting in a shift of the peak below the Fermi energy. The observed increase in the local magnetic moments of Fe(18h) atoms in rh-$Y_2Fe_{17}N_{3.1}$ is well explained in this way. However, the increase in the magnetic moments on the other sites could not be reproduced in our method. Because these sites, except for Fe(9d), are close to N atoms, we concluded that the observed results are produced by nitrogenation. As for Fe(9d) sites, both effects of volume change and nitrogenation could be responsible. Thus, we claim that there are two different mechanisms for the increase in the magnetization and local magnetic moments in rh-$Y_2Fe_{17}N$.

We found that the change in the up-spin local DOS near the Fermi energy affects the magnitude of the MA energy. Detailed calculations of the MA energy for different lattice constants showed that the relation between the MA energy and the electronic states is rather complicated due to the oscillatory energy dependence of MA energy. Nevertheless, it was shown that the lattice constants and local displacement of Fe atoms affect the MA energy rather strongly. Discussions were given on the disagreement between the magnitude of calculated MA energy and experimental one.

ACKNOWLEDGMENTS

This study was supported by the Elements Strategy Initiative Center for Magnetic Materials (ESICMM), Grant No. JPMXP0112101004, through the Ministry of Education, Culture, Sports, Science and Technology (MEXT). Some of the numerical results in this research were obtained using supercomputing resources at Cyberscience Center, Tohoku University.

[1] J. M. D. Coey and H. Sun, J. Magn. Magn. Mater. **87**, L251 (1990).
[2] M. Sagawa, S. Fujimura, N. Togawa, H. Yamamoto, and Y. Matsuura, J. Appl. Phys. **55**, 2083 (1984).
[3] M. Sagawa, S. Fujimura, H. Yamamoto, Y. Matsuura, and S. Hirosawa, J. Appl. Phys. **57**, 4094 (1985).
[4] J. F. Herbst, Rev. Mod. Phys. **63**, 819 (1991).
[5] H.-S. Li and J. M. D. Coey, *Magnetic Materials*, edited by K. H. J. Buschow (North-Holland, Amsterdam, 1991), Vol. 6, p. 1.
[6] J. M. D. Coey and D. P. F. Hurley, J. Magn. Magn. Mater. **104–107**, 1098 (1992).
[7] L. Steinbeck, M. Richter, U. Nitzsche, and H. Eschrig, Phys. Rev. B **53**, 7111 (1996).
[8] M. D. Kuz'min, J. Appl. Phys. **92**, 6693 (2002).
[9] T. Yoshioka and H. Tsuchiura, Appl. Phys. Lett. **112**, 162405 (2018).
[10] H. Tsuchiura, T. Yoshioka, and P. Novák, Scr. Mater. **154**, 248 (2018).
[11] A. V. Andreev, *Handbook of Magnetic Materials*, edited by K. H. J. Buschow (Elsevier Science, Amsterdam, 1995), Vol. 8, p. 59.
[12] K. Koyama and H. Fujii, Phys. Rev. B **61**, 9475 (2000).
[13] A. Teresiak, M. Kubis, N. Mattern, K.-H. Müller, and B. Wolf, J. Alloys Compd. **319**, 168 (2001).
[14] N. Inami, Y. Takeichi, T. Ueno, K. Saito, R. Sagayama, R. Kumai, and K. Ono, J. Appl. Phys. **115**, 17A712 (2014).
[15] S. S. Jaswal, W. B. Yelon, G. C. Hadjipanayis, Y. Z. Wang, and D. J. Sellmyer, Phys. Rev. Lett. **67**, 644 (1991).
[16] M. Ogura, A. Mashiyama, and H. Akai, J. Phys. Soc. Jpn. **84**, 084702 (2015).
[17] J. Kanamori, *Proceedings of 10th International Workshop RE Magnets and Their Applications Kyoto, Japan* (The Society of Non-Traditional Technology, 1989), p.1.
[18] K. Kobayashi, M. Ohmura, Y. Yoshida, and M. Sagawa, J. Magn. Magn. Mater. **247**, 42 (2002).
[19] J. Inoue, H. Nakamura, and H. Yanagihara, T. Mag. Soc. Jpn. **3**, 12 (2019).
[20] J. Inoue, H. Onoda, and H. Yanagihara, J. Phys. D: Appl. Phys. **53**, 195003 (2020).
[21] J. Smit and H. P. J. Wijn, *Ferrite* (Philips Technical Library, Endhoven, 1959).
[22] J. Inoue, J. Phys. D: Appl. Phys. **48**, 445005 (2015).
[23] J. Inoue. T. Yoshioka, and H. Tsuchiura, J. Appl. Phys. **117**, 17C720 (2015).
[24] W. A. Harrison, *Electronic Structure and the Properties of Solids* (Dover, New York, 1980).
[25] J. Inoue and M. Shimizu, J. Phys. F: Met. Phys. **15**, 1511 (1985).
[26] J. Inoue, Physica B **149**, 376 (1988).
[27] F. E. Mabbs and D. J. Machin, *Magnetism and Transition Metal Complexes* (Dover, New York, 2008), p. 30.
[28] A. Sakuma, J. Phys. Soc. Jpn. **63**, 3053 (1994).
[29] R. Haydock, Solid State Phys. **35**, 215 (1980).
[30] V. Heine, W. C. Kok, and C. M. N. Nex, J. Magn. Magn. Mater. **43**, 61 (1984).
[31] E. Abate and H. Asdente, Phys. Rev. **140**, A1303 (1965).
[32] J. Inoue and Y. Ohta, J. Phys. C: Solid State Phys. **20**, 1947 (1987).
[33] J. Inoue, A. Okada, and Y. Ohta, J. Phys. Condens. Matter **5**, L465 (1993).
[34] J. Inoue, T. Yoshioka, and H. Tsuchiura, IEEE Trans. Magn. **55**, 2100304 (2019).
[35] Y. Miura, H. Tsuchiura, and T. Yoshioka, J. Appl. Phys. **115**, 17A765 (2014).
[36] D. Givord, F. Givord, and R. Lemaire, J. de Phys. **32**, C1-668 (1971).
[37] R. Pfranger, D. Plusa, S. Szymura, and B. Wyslocki, Physica B **114**, 212 (1982).
[38] S. Brennan, R. Skomski, O. Cugat, and J. M. P. Coey, J. Magn. Magn. Mater. **140–144**, 971 (1995).
[39] B. Matthaei, J. J. M. Franse, S. Sinnema, and R. J. Radwański, J. de Phys. **49**, C8-533 (1988).
[40] R. Coehoorn, Phys. Rev. B **39**, 13072 (1989).
[41] R. Coehoorn, J. Magn. Magn. Mater. **99**, 55 (1991).
[42] P. Larson, I. I. Mazin, and D. A. Papaconstantopoulos, Phys. Rev. B **67**, 214405 (2003).
[43] R. Skomski, A. Kashyap, A. Solanki, A. Enders, and D. J. Sellmyer, J. Appl. Phys. **107**, 09A735 (2010).

[44] F. Ducastelle and F. Cyrot-Lackmann, J. Phys. Chem. Solid **32**, 285 (1971).
[45] V. Heine and J. H. Samson, J. Phys. F: Metal Phys. **10**, 2609 (1980).
[46] L. Nordström, M. S. S. Brooks, and B. Johansson, J. Magn. Magn. Mater. **104–107**, 1942 (1992).
[47] G. H. O. Daalderop, P. J. Kelly, and M. F. H. Schuurmans, Phys. Rev. B **53**, 14415 (1996).
[48] M. Yamaguchi and S. Asano, J. Magn. Magn. Mater. **168**, 161 (1997).
[49] L. Steinbeck, M. Richter, and H. Eschrig, Phys. Rev. B **63**, 184431 (2001).
[50] J. Schweizer and F. Tasset, J. Phys. F: Met. Phys. **10**, 2799 (1980).
[51] J. M. Alameda, D. Givord, R. Lemaire, and Q. Lu, J. Appl. Phys. **52**, 2079 (1981).
[52] P. Bruno, Phys. Rev. B **39**, 865 (1989).
[53] H. A. Dürr and G. van der Laan, Phys. Rev. B **54**, R760(R) (1996).
[54] Z. Kakol, H. Figiel, and K. Turek, IEEE Trans. Magn. Magn. **20**, 1605 (1984).
[55] D. Koudela, U. Schwarz, H. Rosner, U. Burkhardt, A. Handstein, M. Hanfland, M. D. Kuz'min, I. Opahle, K. Koepernik, K.-H. Müller, and M. Richter, Phys. Rev. B **77**, 024411 (2008).
[56] M. Ochi, R. Arita, M. Matsumoto, H. Kino, and T. Miyake, Phys. Rev. B **91**, 165137 (2015).